Coherent adiabatic theory of two-electron quantum dot molecules in external spin baths

R. Nepstad,[1] L. Sælen,[1,2] and J. P. Hansen[1]
[1]*Department of Physics and Technology, University of Bergen, N-5007 Bergen, Norway*
[2]*Laboratoire de Chimie Physique-Matiére et Rayonnement, Université Pierre et Marie Curie, 11, Rue Pierre et Marie Curie, 75231 Paris Cedex 05, France*
(Received 14 February 2008; published 12 March 2008)

We derive an accurate molecular orbital based expression for the coherent time evolution of a two-electron wave function in a quantum dot molecule where the electrons interact with each other, with external time-dependent electromagnetic fields and with a surrounding nuclear spin reservoir. The theory allows for direct numerical modeling of the decoherence in quantum dots due to hyperfine interactions. Calculations result in good agreement with recent singlet-triplet dephasing experiments by Laird *et al.* [Phys. Rev. Lett. **97**, 056801 (2006)], as well as analytical model calculations. Furthermore, it is shown that using a much faster electric switch than applied in these experiments will transfer the initial state to excited states where the hyperfine singlet-triplet mixing is negligible.

DOI: 10.1103/PhysRevB.77.125315 PACS number(s): 73.21.La, 78.20.Bh, 78.67.−n, 85.35.Be

I. INTRODUCTION

It is now well recognized that the hyperfine interaction is one of the main sources of decoherence in few-electron quantum dots. This interaction, originally considered in metals by Overhauser more than 50 years ago,[1] couples the electronic spin states through weak nuclear spin interactions with an order of $\sim 10^6$ surrounding nuclei.[2] Recently, this coupling has received considerable interest through the demonstration of controlled single-electron manipulation[3,4] which opens for real quantum information processing based on electronic spin states in quantum dots.[5] Procedures to minimize or control the hyperfine interaction are therefore vital for the functioning of any quantum dot based information processing technology. Such mechanisms also contain novel aspects of spin de- and rephasing of quantum systems interacting with a large spin bath.

Recently, it was demonstrated in experiments[6,7] with two-electron quantum dot molecules that the magnitude of the hyperfine interaction is consistent with a random magnetic field strength of a few millitesla. The nuclear field-induced singlet-triplet coupling leads to a spin dephasing of an initially prepared singlet state within 1–10 ns. These experiments utilize fast adiabatic electric switching techniques which transform the ground state from a two-electron ionic state in one dot to a covalent state with one electron in each dot.

The experiments have been analyzed in detail theoretically based on various model Hamiltonians:[8,9] For small tunneling coupling, the effective two-electron Hilbert space amounts to the four possible covalent spin states (a singlet and three triplet states). This may be further reduced to two states by exposing the molecule to a magnetic field which decouples the two states with nonzero magnetic quantum numbers. Within this approximation, it was shown that the hyperfine interaction induces a spin saturation which saturates sensitively as a function of the exchange coupling and the hyperfine coupling.[9] These predictions were confirmed experimentally by Laird *et al.*[10]

In the present paper, we develop a full coherent model of the two-electron spin dynamics which includes the hyperfine interaction on equal footing with the time-dependent external fields. The results may be directly compared with the experimental results. The theory not only validates the effective two-level models in the presence of an external magnetic field but also demonstrates predictive saturation values in the absence of an external magnetic field. Furthermore, it will be shown that decreasing the switching time an order of magnitude may lead to controlled diabatic transfer[11] to excited states where the singlet-triplet mixing can be neglected.

II. MODEL AND COMPUTATIONAL DETAILS

Our starting point is the Hamiltonian of two interacting electrons in a double quantum dot with dot separation d as recently applied in studies of electron structure as well as in studies of photon induced controlled transport.[12–14]

$$\hat{\mathrm{H}} = h(\mathbf{r}_1) + h(\mathbf{r}_2) + \frac{e^2}{4\pi\epsilon_r\epsilon_0 r_{12}}, \tag{1}$$

where

$$\hat{h}(x,y) = -\frac{\hbar^2}{2m^*}\nabla^2 + \frac{1}{2}m^*\omega^2\left[\left(|x| - \frac{d}{2}\right)^2 + y^2\right] + \frac{e^2}{8m^*}B_{ext}^2(x^2+y^2) + \frac{e}{2m^*}B_{ext}L_z + \gamma_e B_{ext}S_z + e\xi(t)x. \tag{2}$$

Here, $\mathbf{r}_{1,2}$ are single-particle coordinates, ξ is an electric time-dependent field applied along the interdot axis, and B_{ext} is an external magnetic field perpendicular to the dot. The material parameters are taken as those of GaAs, with effective mass $m^*=0.067m_e$ and relative permittivity $\epsilon_r=12.4$. The gyromagnetic ratio for GaAs is $\gamma_e=g^*\frac{e}{2m_e}$, with $g^*=-0.44$. The confinement strength is set to $\hbar\omega=1$ meV and the interdot separation to $d=130$ nm, which are realistic experimental values.[4,15]

Figure 1 shows the energy spectrum obtained from diagonalization with $B_{ext}=0$ and $B_{ext}=200$ mT (inset). The spec-

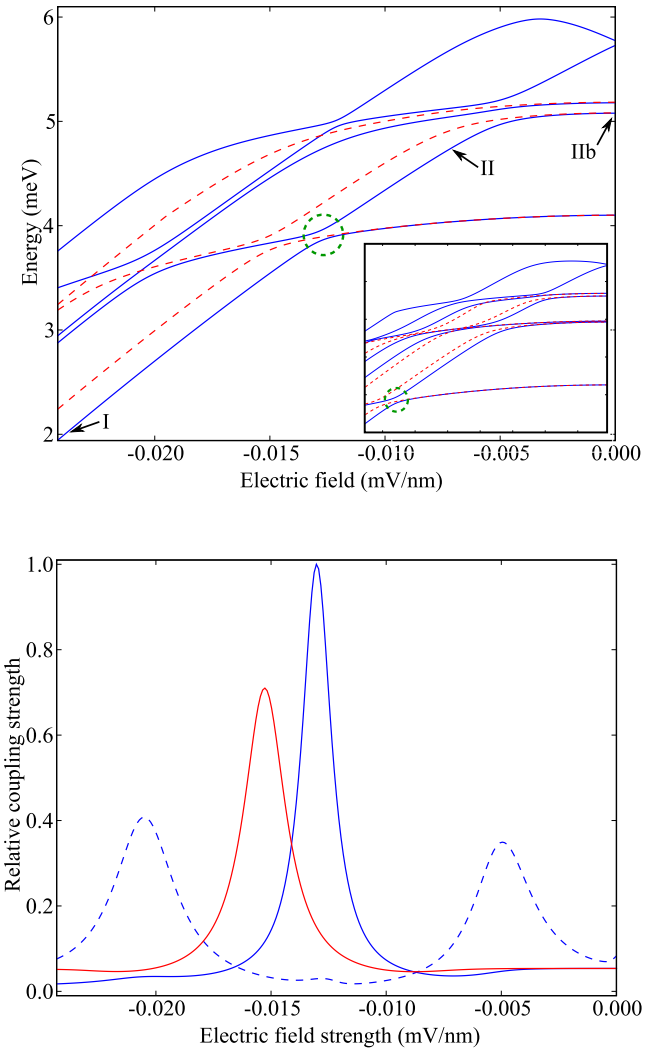

FIG. 1. (Color online) Upper panel shows a few of the lowest energy levels as a function of electric field in the x direction, corresponding to y-symmetric states. The inset shows the effect of an external magnetic field (200 mT) on the spectrum. Lower panel shows the relative coupling strengths of selected states; Full blue/dark gray curve is $\langle 1,S|X|0,S\rangle$ between the ground state and the first excited singlet state (full blue/dark gray curve), full red/gray curve is $\langle 1,T^0|X|0,T^0\rangle$ between the two lowest triplet states, and $\langle 3,S|X|1,S\rangle$ dashed blue/dark gray curve is between the first and third excited singlet states. Note that the $m_s=\pm 1$ triplet states are not shown.

trum of the system has been explained in detail elsewhere;[13] however, we review a few key points here for clarity. Eigenstates are labeled in ascending order according to energy and spin, for instance, $|0,S\rangle$ refers to the singlet ground state. For $B_{ext}=0$, symmetry about the y axis is conserved and we show only singlet and triplet ($m_s=0$) eigenstates with even reflection symmetry. At zero electric field, the energy levels cluster into three distinct "bands" (right axis of Fig. 1). A closer inspection of the eigenstate wave functions reveals certain characteristics common to all the states within a band. In particular, the singlet ground state of the first band may be approximated by linear combination of harmonic oscillator ground state functions centered at $\pm d/2$, forming the so-called covalent states (similarly for the triplet state),

$$|0,S\rangle \propto \phi_{00}(\mathbf{r}_{1L})\phi_{00}(\mathbf{r}_{2R}) + \phi_{00}(\mathbf{r}_{2L})\phi_{00}(\mathbf{r}_{1R}), \tag{3}$$

where $\mathbf{r}_{iL/R}=\mathbf{r}_i \pm \mathbf{d}/2$, $i=1,2$. The subscripts on the harmonic oscillator functions ϕ refer to excitations in the x and y directions, respectively. The states in the second energy band contain a single excitation quantum (n_x^L or n_y^L or n_x^R or $n_y^R=1$) and are of the form (singlets)

$$\phi_{10}(\mathbf{r}_{1L})\phi_{00}(\mathbf{r}_{2R}) + \phi_{00}(\mathbf{r}_{1L})\phi_{10}(\mathbf{r}_{2R}) + \phi_{10}(\mathbf{r}_{1R})\phi_{00}(\mathbf{r}_{2L}) + \phi_{00}(\mathbf{r}_{1R})\phi_{10}(\mathbf{r}_{2L}). \tag{4}$$

Finally, the uppermost states in the third energy band are primarily made up of "ionic" combinations of shifted harmonic oscillator ground state functions, where both electrons occupy the same dot,

$$|3/4,S\rangle \propto \phi_{00}(\mathbf{r}_{1L})\phi_{00}(\mathbf{r}_{2L}) \pm \phi_{00}(\mathbf{r}_{1R})\phi_{00}(\mathbf{r}_{2R}). \tag{5}$$

When an external magnetic field is applied, the y symmetry is broken and all states are shown (inset of Fig. 1). The magnetic sublevels also split, but this is not shown. For the relatively weak magnetic fields considered here, the description above is still valid. However, in addition to the splitting of the spin states (anomalous Zeeman effect), the spectrum is also changed by the Zeeman (L_z) and diamagnetic (B_{ext}^2) terms, as seen clearly in the inset. The most important effects of these terms are the modified singlet-triplet splitting J, the modified anticrossing energy difference (green dashed circle), and the splitting of the second band according to the sign of the angular momentum expectation value $\langle L_z\rangle$.

It is particularly worth noting that the energy spectrum exhibits several near degenerate anticrossing regions where the coupling strength can be tuned in experiments through adjustable gate voltages and switching times.[10] Restricted by conservation of total spin, the states can couple dynamically as the electric field varies. The relative coupling strength from our model is shown in the lower panel of Fig. 1. The strongest coupling strength is seen between the singlet ground state and first excited states at -0.013 mV/nm. This sets a limit on the switching time through the region enclosed by a green dashed circle for adiabatic time development along the initial singlet ground state, marked as I in Fig. 1. On the other hand, a very rapid transfer can lead to diabatic development, to be discussed later.

The few and well defined states resulting from the present diagonalization suggest that the time evolution is most precisely described in an adiabatic basis of instant eigenstates of the time-dependent Hamiltonian of Eq. (1), $\hat{H}(t)\chi(\mathbf{r}_1,\mathbf{r}_2;\xi) = \epsilon(\xi)\chi(\mathbf{r}_1,\mathbf{r}_2;\xi)$, where the energies $\epsilon(\xi)$ depend parametrically on the time-dependent electric field. We expand the wave function in these basis states,

$$\Psi(\mathbf{r}_1,\mathbf{r}_2,t) = \sum_k c_k(t)\chi_k(\mathbf{r}_1,\mathbf{r}_2;\xi)\otimes|S\rangle, \tag{6}$$

where k runs over all basis states. Projecting onto each basis state, the following expression for the time evolution of the amplitudes is obtained,

$$\dot{c}_k(t) = \dot{\xi} \sum_{j \neq k} \frac{\langle \chi_k | X | \chi_j \rangle}{\epsilon_k - \epsilon_j} c_j(t) + i\epsilon_k(\xi) c_k(t), \tag{7}$$

with $X = x_1 + x_2$.

Additional terms can readily be included as extra matrix elements in the expression above. To study hyperfine interactions, spin couplings for $\sim 10^6$ nuclear spins surrounding the electrons must be included. These evolve in time, but on a much longer time scale than we will consider here. We therefore use the quasistatic approximation,[8,16] neglecting their time dependence. In addition, the large number of spins justifies a semiclassical approximation,[17] where all the nuclear spins are described by a single classical magnetic field. The hyperfine interaction is then given by

$$\hat{H}_N = \gamma_e \sum_{i=1,2} \mathbf{S}_i \cdot \mathbf{B}_N(r_i), \tag{8}$$

where S_i is the spin operator of electron i. Generally, the direction of nuclear magnetic field $\mathbf{B}_N$ is random (no polarization) and the magnitude varies according to a normal distribution about zero, $P(\mathbf{B}_N) = 1/(2\pi B_{\text{nuc}}^2)^{3/2} \times \exp(-\mathbf{B}_N \cdot \mathbf{B}_N / 2B_{\text{nuc}}^2)$.[9] B_{nuc} can be determined by experiments and is of the order of 1 mT.[4] The precise spatial variation of the nuclear magnetic field $\mathbf{B}_N$ is, in general, unknown and also of less importance. The essential feature in the spin-dephasing mechanism is the difference in effective magnetic fields between the two dots. The simplest way to represent this is by a step function,

$$\mathbf{B}_N = \begin{cases} (B_x \hat{\mathbf{e}}_x + B_y \hat{\mathbf{e}}_y + B_z \hat{\mathbf{e}}_z) & \text{for } x \geq 0 \\ 0 & \text{otherwise.} \end{cases} \tag{9}$$

This induces coupling between the singlet and triplet states and between the different triplet states.

From Eqs. (1), (6), and (9), the time evolution of the wave function at zero electric field, restricted to the four lowest energy states $\{|S\rangle, |T^0\rangle, |T^-\rangle, |T^+\rangle\}$, becomes,

$$\dot{\mathbf{c}}(t) = \imath\gamma_e \begin{pmatrix} J/\gamma_e & B_z & \frac{B_x - \imath B_y}{\sqrt{2}} & -\frac{B_x + \imath B_y}{\sqrt{2}} \\ B_z & 0 & 0 & 0 \\ \frac{B_x + \imath B_y}{\sqrt{2}} & 0 & -B_{ext} & 0 \\ -\frac{B_x - \imath B_y}{\sqrt{2}} & 0 & 0 & B_{ext} \end{pmatrix} \mathbf{c}(t). \tag{10}$$

This expression is identical to four-level models previously considered.[8] We have here, however, excluded the inter triplet couplings as this will allow us to obtain an analytical solution. When the external magnetic field is sufficiently strong, the $m_s = \pm 1$ triplet components effectively decouple, and we are left with a two-level system defined by the upper left part of the four-level matrix. Furthermore, since the triplet sublevels are degenerate, the four-level matrix for $B_{ext} = 0$ may be represented by an effective "radial" two-level model. In both cases, we obtain the time evolution of the singlet coefficient,

$$|c_S(t)|^2 = 1 - \frac{4B^2}{4B^2 + J^2} \sin^2\left(\frac{1}{2} t \sqrt{4B^2 + J^2}\right), \tag{11}$$

with $B = B_z$ for $B_{ext} \gg J$ and $B = \sqrt{B_x^2 + B_y^2 + B_z^2}$ for $B_{ext} = 0$.

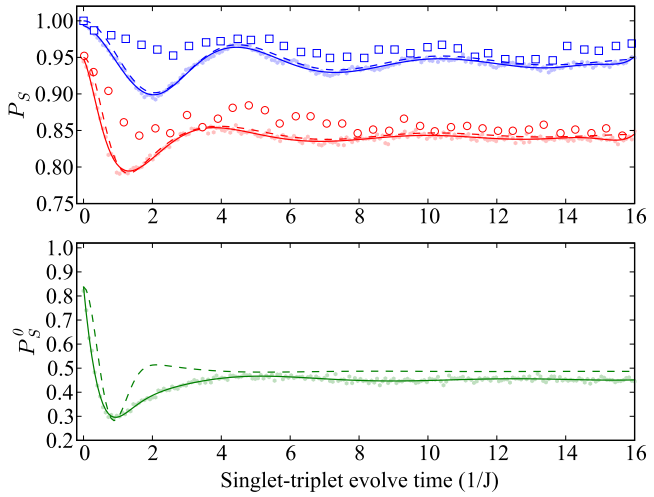

FIG. 2. (Color online) Upper panel: averaged time evolution of singlet component with $B_{ext} = 200$ mT. $B_N/J = 0.4$ (full blue/dark gray line) and $B_N/J = 0.91$ (full red/gray line, downshifted 5%). Squares and circles are experimental data taken from Ref. 10. Prediction from two-level model shown as dashed lines. Semitransparent dots are actual numerical data; full lines are obtained from a smoothed spline interpolation. Lower panel: $B_N/J = 0.91$, but without external magnetic field. Prediction from four-level model (dashed line), scaled to match at $t = 0$.

III. RESULTS AND DISCUSSION

In Fig. 2, we show our results together with experimental results of Laird *et al.*[10] using $B_{ext} = 200$ mT (upper panel). To calculate the singlet-triplet dephasing, we start out in the singlet ground state at large electric field, −0.024 mV/nm. The field is then switched adiabatically to zero within 1 ns and kept at zero a variable period of time, t_s up to $16J/\hbar$ ns, before being switched back to its original value. The procedure is repeated a number of times, with a random nuclear magnetic field drawn from a Gaussian distribution. Finally, the average of the singlet correlator is computed, $P_S = 1/N \Sigma_i |c_S^i(t_s)|^2$. The full lines in the upper ($B_{ext} = 200$ mT) and lower panels ($B_{ext} = 0$) of Fig. 2 are produced from a sample size of $N = 1000$ different nuclear fields. For clarity, we have interpolated the numerical data using splines with a smoothing requirement. The actual numerical points are shown as semitransparent dots. Also shown, as dashed lines, are predictions from the two-level theory. An excellent agreement between the theoretical results is noted, which indicate that effects of the electrical switch, excited states, and geometry of the potential are of less importance in this case. The present results are also compared with experimental data, shown as dots and circles in the upper panel. We also observe a very good agreement with the experimental

results. Here, we have varied B_{nuc} as opposed to J which may be varied in experiments by tuning the gate voltages. As verified by the two-level models, the dephasing process mainly relies on their ratio. It should be noted that results in the upper panel have been scaled according to $P_S(t)=1-V[1-P_S^0(t)]$, where $V=0.40$ is a visibility parameter determined in the experiments, $P_S(t)$ is the experimental averaged correlator, and $P_S^0(t)$ is the theoretical averaged correlator.[10]

Setting the external magnetic field to zero leads to increased dephasing, since the $m_s=\pm 1$ states are now coupled to the initial singlet state. This is indeed what we observe in our simulations, as shown in the lower panel of Fig. 2. The four-level (effective two-level) model yields the result shown as a dashed line, scaled to match the numerical data at $t_s=0$. At large evolve times, these are in good agreement. Numerical solution of the full four-level matrix suggests that the slight discrepancy around $t_s=2$ is due to the neglected inter-triplet couplings in Eq. (10). In contrast to the two-level case, we observe in the four-level case an $\sim 10\%$ dephasing occurring during the switch or more precisely between the two passages of the avoided crossing circled out in Fig. 1. This is a result of a much more involved dynamical interplay between the states and result in the present theory to a reduction of P_S^0 at $t_s=0$.

An interesting feature can be studied by introducing an ultrafast switching function which leads to diabatic passage through the anticrossing, highlighted by the green dashed circle in Fig. 1. This will transfer the system to the first excited singlet state where at zero electric field, the singlet-triplet splitting is approximately 100 times greater compared to the ground state. It is important to note that states in the second energy band are like the ground state covalent states[13] with one electron in each dot. This makes the states well suited for single-electron gate operations, unlike the states in the third energy band, which resemble ionic states. In Fig. 3, the evolution of the three lowest energy singlet states is displayed as the system is rapidly switched from positions marked I and II in Fig. 1 using a nuclear magnetic field of 1 mT and zero external magnetic field. From there, it is transferred adiabatically from II to IIb. The leftmost panel shows the transfer of population from the ground to first excited state during a 1 ps switch, with around 10% of the population being further transported to the second excited state. In the middle panel, the system is switched adiabatically to zero electric field during 2 ns and left to evolve here for 50 ns. The singlet-triplet coupling is completely suppressed, and when the system is switched back to position I, 95% of the initial singlet population is regained, the rest having vanished mostly to higher excited states during passage through the anticrossings. The simulation was repeated a number of times with increasing nuclear magnetic field strength of up to 10 mT, attributing only negligible changes to the dynamics. We note that by applying optimal control schemes, the transition to excited states may be achieved with near 100% transition probability.[11,12,18]

Finally, some comments on the harmonic double-dot potential [Eq. (2)] is appropriate. Perturbations of this potential, such as asymmetry or nonparabolic shape, may be included in order to achieve a better correspondence with physical double dots. However, for the few lowest energy states which we have considered in this paper, small perturbations only cause small alterations in the energy spectrum. The dynamical properties we have studied will therefore remain essentially unchanged, as seen by the good agreement with experimental results (see Fig. 2).

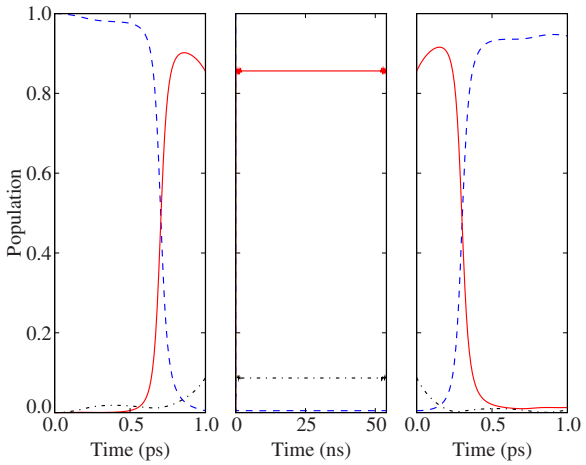

FIG. 3. (Color online) The time evolution of the three most prominent states during the fast switch procedure. About 95% of the total norm is represented by these states, which are $|S,0\rangle$ (blue/dark gray dashed line), $|S,1\rangle$ (red/gray full line), and $|S,2\rangle$ (black dash dotted line). $B_{\mathrm{nuc}}=1$ mT ([1,1,1]). $B_{ext}=0$. The left panel shows the evolution during rapid switch (1 ps); center panel shows adiabatic passage to first excited state and evolution during dephasing period. Right panel shows rapid switching back to the one-dot configuration (1 ps). Singlet-triplet coupling is weak for the excited singlet state and thus only $\sim 5\%$ is lost (mainly to other singlet states during switching).

IV. CONCLUSION

In conclusion, we have applied a first principles molecular orbital framework to accurately calculate the time development of the electronic states of a two-electron quantum dot molecule. The hyperfine interaction has been taken into account on the same coherent level as the time variation of the external electromagnetic fields. Calculations have displayed a very good agreement with experiments and a previously developed two-level model for experiments performed in static external magnetic fields. We have also performed full numerical calculations in the absence of external magnetic field and predicted the dephasing dynamics by an effective four-level model. Finally, we have pointed toward a solution to the spin-dephasing problem by controlling and applying transitions between excited states.

ACKNOWLEDGMENTS

This research has been supported by the Research Council of Norway (RCN). L.S. acknowledges financial support through a mobility grant from Université Pierre et Marie Curie.

[1] A. W. Overhauser, Phys. Rev. **92**, 411 (1953).
[2] A. V. Khaetskii, D. Loss, and L. Glazman, Phys. Rev. Lett. **88**, 186802 (2002).
[3] F. H. L. Koppens, C. Buizert, K. J. Tielrooij, I. T. Vink, K. C. Nowack, T. Meunier, L. P. Kouwenhoven, and L. M. K. Vandersypen, Nature (London) **442**, 766 (2006).
[4] J. R. Petta, A. C. Johnson, C. M. Marcus, M. P. Hanson, and A. C. Gossard, Phys. Rev. Lett. **93**, 186802 (2004).
[5] D. Loss and D. P. DiVincenzo, Phys. Rev. A **57**, 120 (1998).
[6] F. H. L. Koppens, J. A. Folk, J. M. Elzerman, R. Hanson, L. H. W. van Beveren, I. T. Vink, H. P. Tranitz, W. Wegscheider, L. P. Kouwenhoven, and L. M. K. Vandersypen, Science **309**, 1346 (2005).
[7] J. R. Petta, A. C. Johnson, J. M. Taylor, E. A. Laird, A. Yacoby, M. D. Lukin, C. M. Marcus, M. P. Hanson, and A. C. Gossard, Science **309**, 2180 (2005).
[8] J. M. Taylor, J. R. Petta, A. C. Johnson, A. Yacoby, C. M. Marcus, and M. D. Lukin, Phys. Rev. B **76**, 035315 (2007).
[9] W. A. Coish and D. Loss, Phys. Rev. B **72**, 125337 (2005).
[10] E. A. Laird, J. R. Petta, A. C. Johnson, C. M. Marcus, A. Yacoby, M. P. Hanson, and A. C. Gossard, Phys. Rev. Lett. **97**, 056801 (2006).
[11] G. E. Murgida, D. A. Wisniacki, and P. I. Tamborenea, Phys. Rev. Lett. **99**, 036806 (2007).
[12] L. Sælen, R. Nepstad, I. Degani, and J. P. Hansen, Phys. Rev. Lett. **100**, 046805 (2008).
[13] V. Popsueva, R. Nepstad, T. Birkeland, M. Førre, J. P. Hansen, E. Lindroth, and E. Walterson, Phys. Rev. B **76**, 035303 (2007).
[14] A. Harju, S. Siljamaki, and R. M. Nieminen, Phys. Rev. Lett. **88**, 226804 (2002).
[15] D. M. Zumbühl, C. M. Marcus, M. P. Hanson, and A. C. Gossard, Phys. Rev. Lett. **93**, 256801 (2004).
[16] I. A. Merkulov, A. L. Efros, and M. Rosen, Phys. Rev. B **65**, 205309 (2002).
[17] J. S. Briggs and J. M. Rost, Eur. Phys. J. D **10**, 311 (2000).
[18] E. Räsänen, A. Castro, J. Werschnik, A. Rubio, and E. K. U. Gross, Phys. Rev. Lett. **98**, 157404 (2007).